



Changes in tropical cyclones under stabilized 1.5 and 2.0 °C global warming scenarios as simulated by the Community Atmospheric Model under the HAPPI protocols

Michael F. Wehner¹, Kevin A. Reed², Burlen Loring¹, Dáithí Stone¹, and Harinarayan Krishnan¹

¹Lawrence Berkeley National Laboratory, Berkeley, California 94720, USA

²State University of New York at Stony Brook, Stony Brook, New York 11794, USA

Correspondence: Michael F. Wehner (mfwehner@lbl.gov)

Received: 31 October 2017 – Discussion started: 6 November 2017

Accepted: 17 January 2018 – Published: 28 February 2018

Abstract. The United Nations Framework Convention on Climate Change (UNFCCC) invited the scientific community to explore the impacts of a world in which anthropogenic global warming is stabilized at only 1.5 °C above preindustrial average temperatures. We present a projection of future tropical cyclone statistics for both 1.5 and 2.0 °C stabilized warming scenarios with direct numerical simulation using a high-resolution global climate model. As in similar projections at higher warming levels, we find that even at these low warming levels the most intense tropical cyclones become more frequent and more intense, while simultaneously the frequency of weaker tropical storms is decreased. We also conclude that in the 1.5 °C stabilization, the effect of aerosol forcing changes complicates the interpretation of greenhouse gas forcing changes.

1 Introduction

Changes in tropical cyclone intensity, frequency and distribution are expected as the climate warms due to anthropogenic changes in the composition of the atmosphere. While the development of a complete climate theory of tropical cyclones remains elusive (Walsh et al., 2015), recent advances in high-performance computing enable multi-decadal simulations of climate models at tropical-cyclone-permitting resolutions. Together with conceptual models, such numerical models are the tool of choice for investigating projected future changes in tropical cyclones (Wehner et al., 2017a).

Previous work has studied the impact of climate change on tropical storms through idealized representations of future climate through uniform increases in greenhouse gases and sea surface temperature (Walsh et al., 2015; Wehner et al., 2015) or more realistic but more extreme cases of warming using the Representative Concentration Pathway (RCP4.5 or RCP8.5) scenarios (e.g., Camargo, 2013; Knutson et al., 2015; Bacmeister et al., 2018). The United Nations Frame-

work Convention on Climate Change (UNFCCC) invited the International Panel on Climate Change (IPCC) to explore the impacts of a world in which the expected average warming remains less than or equal to 2.0 °C over preindustrial levels. In particular, the UNFCCC requested an analysis of the feasibility and impacts of a target stabilized global mean temperature of 1.5 °C over preindustrial levels. The Half a degree Additional warming, Prognosis and Projected Impacts (HAPPI) experimental protocol was designed in response to this request to permit a comparison of the effects of stabilizing anthropogenic global warming at 1.5 °C over preindustrial levels to 2.0 °C (Mitchell et al., 2017). In this paper, we present results from a high-resolution atmosphere–land model forced by the HAPPI prescriptions of sea surface temperature (SST) and sea ice concentration.

The HAPPI experimental protocol consists of three parts (Mitchell et al., 2017). The “historical” part specifies observed sea surface temperatures (SSTs) from the NOAA OI.v2 gridded monthly mean observational product (Reynolds et al., 2002) over the period 1996–2015.

An estimate of SST and sea ice concentrations in stabilized scenarios at both 1.5 and 2.0 °C is constructed from the CMIP5 (Coupled Model Intercomparison Project) multi-model database of future climate projections under the RCP2.6 and RCP4.5 forcing scenarios hereafter designated “HAPPI15” and “HAPPI20”. A stabilized anthropogenic climate change to these surface forcing functions is constant in time. By adding such a change to the observations, observed interannual variations are preserved. As such, historical year 2006 is directly comparable to HAPPI15 or HAPPI20 year 2106 as the date in the stabilized scenarios is arbitrarily increased by 1 century. The original design of the HAPPI protocols follows that of the “Climate of the 20th Century Plus Detection and Attribution project” (C20C+) (Stone et al., 2017) and targets large ensembles of 50 realizations or more to quantify the differences in projections (or attribution) of extreme events in specific years. However, at the high horizontal resolutions necessary to simulate tropical cyclones, the computational costs of the climate model are too high to permit such a large number of simulations and ensemble sizes are restricted. Hence, in this study we pool results across both simulation years and the ensembles for each part of the HAPPI experiment to isolate the climate change signal, if any, from internal variability. As part of our participation in the C20C+ project, we began the historical simulation period in 1996 extending through 2015, thus permitting a more robust estimate of present day simulated tropical cyclone statistics for comparison to the stabilized warmer climate.

This study uses the Community Atmospheric Model version 5.3 configured at a global resolution of approximately 0.25°, roughly equaling a grid spacing of 28 km in tropical regions. Note that this participating model is listed as “CAM5.1.2-0.25degree” in the HAPPI documentation (<http://portal.nersc.gov/c20c/data.html>), but here it is abbreviated to “CAM5”. This configuration has been demonstrated to produce reasonable annual numbers of tropical cyclones on the global scale compared to observations (Bacmeister et al., 2014; Wehner et al., 2014; Reed et al., 2015). The formulation of the dynamical core portion of the atmospheric model does influence tropical cyclone counts and intensities (Reed et al., 2015). The model used in this study used CAM5’s finite-volume-based dynamical core on a latitude–longitude grid (Lin and Rood, 1996, 1997; Lin, 2004). Storms up to category 5 on the Saffir–Simpson scale are regularly produced, allowing for investigation into the effects of global warming on the distribution of tropical cyclone intensity. The relationship between maximum wind speed and central pressure minima was also demonstrated to be realistic (Wehner et al., 2014). However, there are significant biases in track and cyclogenesis density, particularly in the Pacific Ocean with the model simulating too many storms in the central North Pacific and too few in the northwestern part of that basin.

Nonetheless, the high-resolution CAM5 can be an informative tool to explore the change in tropical cyclone behavior in altered climates. Wehner et al. (2015) explored tropical cy-

clone behavior in the four idealized climate change configurations of the US CLIVAR Hurricane Working Group (Walsh et al., 2015). That project compared the combined effect of a spatially uniform 2 °C increase applied to a climatological average of observed SST centered at 1990 and of a doubling of atmospheric CO₂ to a control 1990 simulation, as well as the separate effects of each factor. Their principal finding was that a lower-resolution (1°) version of the CAM5 and methods based on the genesis potential index (Emanuel and Nolan, 2004) could not reproduce the sign of the change in the global number of tropical cyclones produced by the high-resolution version. Under the combined effect of the uniform 2 °C SST increase and CO₂ doubling, the high-resolution CAM5 reduced the annual number of tropical storms (category 0–5) from 86 ± 4 to 70 ± 3. However, the annual number of intense tropical cyclones (category 4–5) increased from 10 ± 1.7 to 12 ± 1.7. The two separate forcing simulations revealed that most of the reduction in the total number of tropical storms of all intensities was caused by the change in the vertical temperature profile due to the CO₂ doubling, while the increase in the number of intense tropical cyclones was caused solely by the increased SST. The warmer SST conditions also caused the maximum wind speeds of the most intense storms to increase and their central pressure minima to decrease, while CO₂ doubling had the opposite effect. The peak of the zonally averaged tropical storm track density shifted poleward by ~ 2° in the Northern Hemisphere and ~ 4° in the Southern Hemisphere in all three perturbed US CLIVAR configurations. A small poleward shift (~ 1°) in Northern Hemisphere cyclogenesis origins was exhibited in the two simulations with warmer SSTs but not the CO₂ doubling only simulation, while all three perturbed simulations exhibited a similar shift in the broader Southern Hemisphere cyclogenesis distribution.

The SST and sea ice perturbations imposed by the HAPPI protocols exhibit the more realistic spatially varying SST patterns shown in Fig. 1 than the uniform increase in the US CLIVAR experiments. In the HAPPI protocols, warmer configurations are produced by adding monthly climatological perturbations to the observed SSTs for each individual month, preserving the current patterns of SST variability. The SST perturbations for the 1.5 °C stabilization scenario are taken directly from the multi-model mean of CMIP5 RCP2.6 simulations (which conveniently warm by approximately that amount on average above preindustrial temperatures). Radiative forcings (greenhouse gas concentrations, burdens of various aerosol species and ozone concentrations) are also taken directly from the RCP2.6 values. The 2.0 °C scenario uses SST perturbations and CO₂ concentrations interpolated between CMIP5 RCP2.6 and RCP4.5 multi-model means, while other forcings remain the same as for the 1.5 °C scenario. Sea ice concentrations are computed using an adapted version of the method described in Massey (2018) by using observations of SST and ice to establish a linear relationship between the two fields for the time period 1996–2015 and

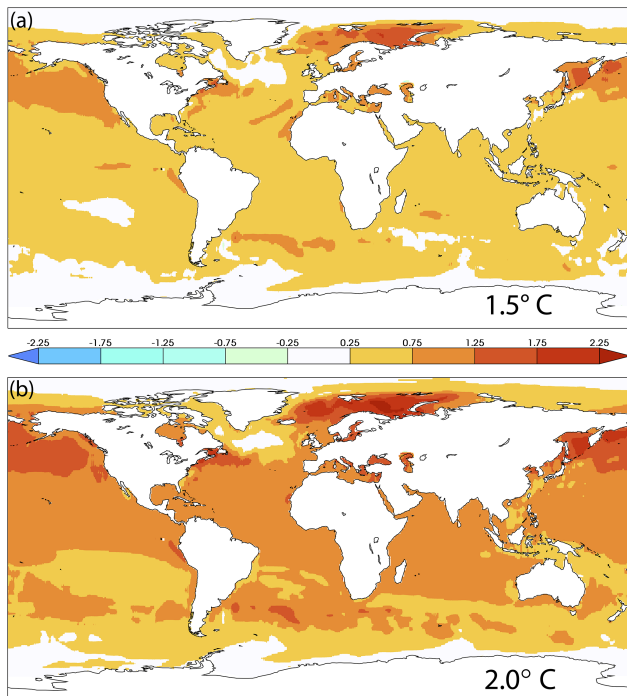


Figure 1. The temporal average of the imposed change ($^{\circ}\text{C}$) in sea surface temperature as prescribed by the HAPPI protocols: (a) 1.5°C stabilization, (b) 2.0°C stabilization.

are consistent with the HAPPI prescribed SST fields. Details are further described in Mitchell et al. (2017). Although they represent a smaller perturbation to the climate system than the US CLIVAR experiment, the HAPPI experiment is more physically consistent in terms of the relationship of the SST change to radiative forcing changes and in the distribution of sea ice in the high latitudes, permitting the HAPPI simulations to be more widely applicable to phenomena outside of the tropics.

The CAM5 simulations performed for the HAPPI project consist of five realizations of the historical period plus six realizations of each stabilization scenario. One of the historical realizations is incomplete due to computer resource limitations, resulting in 96 simulated years for this part of the dataset. Sixty simulated years were produced for both the 1.5 and 2.0°C stabilization scenarios. Data products are freely available with further information provided at www.portal.nersc.gov/c20c. Simulated tropical cyclones are identified and tracked with the Toolkit for Extreme Climate Analysis (TECA2.) available for download and installation at <https://github.com/LBL-EESA/TECA> using the methods described in Knutson et al. (2007).

Another critical difference between the HAPPI and the US CLIVAR experimental protocols is the aerosol forcing. While the US CLIVAR protocols had no specified changes to aerosols, the HAPPI protocols set aerosol forcings to the end of the 21st century levels under the RCP2.6 scenario

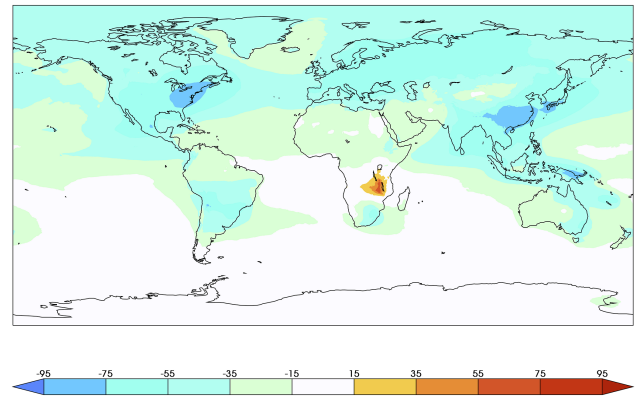


Figure 2. Percent difference between the stabilized 2°C scenario and the historical simulation of the total aerosol optical depth in the visible band.

for both stabilization scenarios. Hence, there is a substantial reduction in the aerosol forcing in the stabilization simulations compared to the historical simulations. Dunstone et al. (2013) indirectly found a substantial reduction in Atlantic tropical storms by varying aerosol forcing in the UK MetOffice climate model HadGEM2-ES at a resolution of $1.2^{\circ} \times 1.9^{\circ}$. In the CAM5 simulations presented here, we used its bulk aerosol model to prescribe aerosol concentrations rather than emissions in order to reduce the computational burden (Kiehl et al., 2000). Huff et al. (2017) established that CAM5 does exhibit sensitivity to aerosol formulation in the simulated number and intensity distribution of tropical cyclones in the simulated current climate. However, the HAPPI protocol does not establish a controlled investigation of the effects of the aerosol forcing reduction in the stabilized scenarios, nor have we performed such simulations yet. Figure 2 shows the percent change in total aerosol optical depth in the visible band comparing the historical and 2.0°C stabilization simulations averaged over all years and realizations. Significant decreases are evident over most of the Northern Hemisphere and the tropics. Results from the 1.5°C stabilization simulations are the same.

2 Results

As in the US CLIVAR idealized experiments, the global number of intense tropical cyclones (category 4 and 5) is substantially increased in the warmer climates of the HAPPI stabilization scenarios, with a statistical significance higher than the 1% level as shown in Fig. 3. Also as in the idealized warming experiments, the number of tropical storms (category 0) is substantially decreased in a warmer climate. However, the effect on the total number of named storms of all intensities (category 0–5) is subtler in the HAPPI simulations. For this version of CAM5, the global annual number of category 0 to 5 storms is 73.4 ± 0.91 in the historical en-

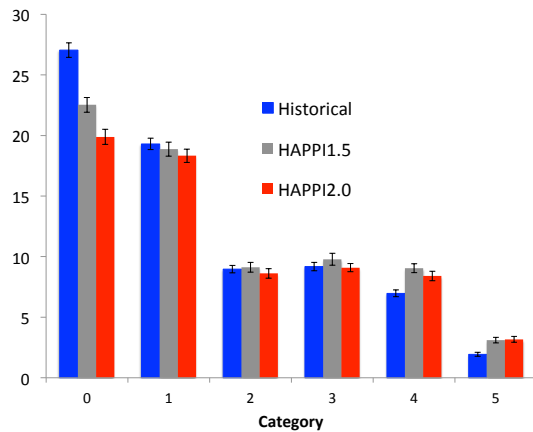


Figure 3. Global annual number of tropical cyclones by Saffir–Simpson scale for the historical (blue), 1.5 °C stabilization scenario (gray) and 2 °C stabilization scenario (red). Error bars are the standard errors based on interannual variability. Blue: historical. Gray: 1.5° stabilization. Red: 2.0° stabilization.

semble¹. In the 1.5 °C stabilization scenario, this number is only reduced to 72.5 ± 1.2 , which is not significant at a 10 % significance level. However, in the 2.0 °C stabilization scenario, a further reduction to 67.5 ± 1.3 is realized, which is significant at the 1 % level. In the cooler stabilization scenario, the decrease in category 0 storms is roughly offset by the increase in intense storms, leading to the insignificance of the change in the total number of storms. In the warmer scenario, the yet larger decrease in category 0 causes the change in the total number of storms to be more significant. In both stabilization scenarios, the changes from the historical simulation in category 1, 2 and 3 storms are not statistically significant above the 5 % level. Differences between the 1.5 and 2 °C stabilization scenarios are only highly significant in the decrease by category for the number of the weakest category of storms. Importantly, the differences in the number of intense tropical cyclones between the two warming scenarios are not statistically significant in this study. The results presented in Fig. 3 are repeated numerically in Table 1. Basin-specific results are tabulated in the Supplement.

Average storm track length, duration and mean translational speed are shown for the HAPPI scenarios as a function of maximum lifetime intensity on the Saffir–Simpson scale in Fig. 4. Weak storms (category 0) show no substantial changes in track length, translational speed or duration among the three ensembles of CAM5 simulations and this result is consistent with the US CLIVAR experiments (Wehner et al., 2015). While these three metrics show increases for

¹The historical annual global tropical storm counts over all categories differ from the 1990 climatological simulations of Wehner et al. (2015) for three reasons: (1) SSTs are slightly different, (2) the version of CAM5 is a more recent release (CESM v1.2.2 vs. v1.0.3) and (3) there are subtle differences in the implementation of the tracking algorithm.

category 2–4 storms in the 1.5 °C stabilization scenario compared to the historical simulations, those increases are attenuated in the warmer 2.0 °C stabilization scenario. However, the most intense storms (category 5) exhibit consistent increases in track length and duration on average as the climate system warms. Translational speed (here averaged over the entire storm duration) increases in all three ensembles with storm intensity but the differences among scenarios are complex. Notably, while increases in average translational speed in the warmer scenarios are simulated for storms in the middle of the Saffir–Simpson scale, decreases are simulated for the most intense category. While all of the differences in Fig. 4 are statistically significant well above the 1 % level due to the large number of storms tracked, subtle changes in the experimental design, including changes in SST pattern or aerosol forcing, might alter these results. Better quantification of this type of structural uncertainty will require further developments in high-performance computing technologies to permit more diverse experiments.

The zonal average of the normalized density of storm tracks of all intensities for the HAPPI scenarios is shown in Fig. 5a. As mentioned above, CAM5 is known to have a significant bias in the genesis location of Pacific tropical storms although the total number, both in that basin and globally, is not far from observed records. More detailed but somewhat noisy maps of track density differences among the HAPPI scenarios are shown Fig. S1 in the Supplement. Integrating over all longitudes, as in Fig. 5, damps this noise, revealing a poleward shift in the warmer HAPPI scenarios compared to the historical simulations. In the Northern Hemisphere, there is a tendency for a substantially larger normalized density of storm tracks poleward of 25° N in both the Atlantic and Pacific Ocean basins (see Fig. S1). This may partially explain the increased track lengths and durations shown in Fig. 4. With warmer temperatures, conditions that can sustain tropical storm wind speeds extend poleward. Although not considered here, there is potential for an anthropogenic influence on the transition to extratropical characteristics of storms that undergo them (Liu et al., 2017; Zarzycki et al., 2017). In the Southern Hemisphere, Fig. 5 reveals that normalized storm track density is a narrower function of latitude in the warmer HAPPI scenarios. Figure S1 reveals that this is mainly due to a change in the location of simulated tropical storms in the southern Indian Ocean. In both hemispheres, differences between the 1.5 and 2.0 °C stabilization scenarios are smaller and noisier, making any differences in track density between them difficult to interpret. The statistical significance of the larger differences in normalized track density between the historical and warmer stabilized scenarios is very high as assessed by a comparison of the standard errors.

The zonal average of the normalized cyclogenesis density for tropical storms of all intensities is shown in Fig. 5b. Again, more detailed but noisy maps of cyclogenesis density differences among the HAPPI scenarios are shown in Fig. S2. In the Northern Hemisphere, a much smaller poleward shift

Table 1. Differences in CAM5 simulated global annual tropical storm counts by Saffir–Simpson scale between the two HAPPI stabilization scenarios, the historical simulation and each other. Differences that are statistically significant at the 1 % level are in bold, while those at the 10 % level are in italics.

Saffir–Simpson	0–5	0	1	2	3	4	5
HAPPI15 minus historical	−0.9	−4.5	−0.4	0.2	0.6	2.1	1.2
HAPPI20 minus historical	−5.9	−7.2	<i>−1.0</i>	−0.4	−0.1	1.4	1.2
HAPPI20 minus HAPPI15	−5.0	−2.6	−0.5	−0.5	−0.7	−0.6	0.1

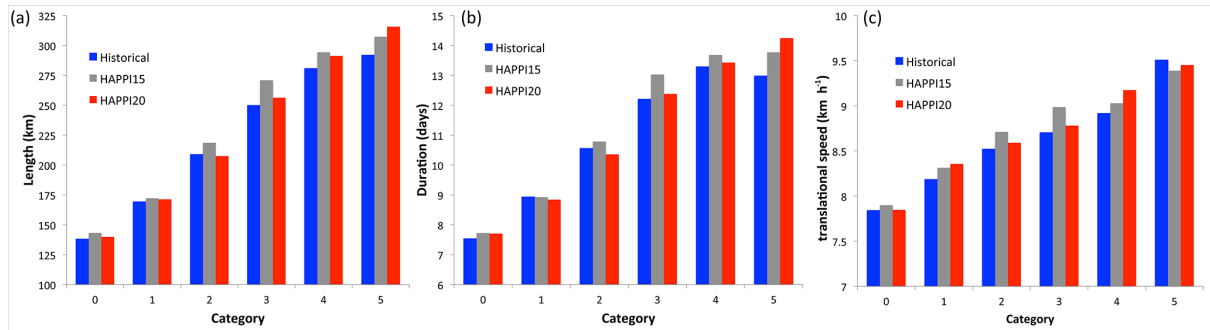


Figure 4. (a) Average tropical storm track length (km) for the HAPPI scenarios as a function of maximum intensity on the Saffir–Simpson scale. (b) Average tropical storm track duration (days) for the HAPPI scenarios as a function of maximum intensity on the Saffir–Simpson scale. (c) Average tropical storm track speed (km h^{-1}) for the HAPPI scenarios as a function of maximum intensity on the Saffir–Simpson scale. Blue: historical. Gray: 1.5° stabilization. Red: 2.0° stabilization.

than for track density starting at about 15°N is simulated in the warmer HAPPI scenarios compared to the historical simulations. Figure S2 suggests that much of this change is coming from the Atlantic Ocean, but these cyclogenesis differences are not as compelling as they are for the tropical storm tracks. In the Southern Hemisphere, the cyclogenesis changes are similar to the track changes in both Fig. 5 and the Supplement. Hence, we can conclude that the shifts in Southern Hemisphere tracks are mainly a result of cyclogenesis shifts that are mostly in the southern Indian Ocean.

The annual accumulated cyclonic energy (ACE) is shown in Fig. 6 for the historical and HAPPI stabilization scenarios both globally and by the major ocean basins with tropical cyclone activity. ACE is a measure of the annual kinetic energy contained in tropical storms and is obtained by squaring the maximum sustained surface wind in the system every 6 h and summing it up for the year (http://www.cpc.ncep.noaa.gov/products/outlooks/background_information.shtml). Comparison with an observational estimate taken from Maue (2011) suggests that the model is overactive by this measure of tropical cyclone activity, although differences in the methods with which tracks and wind speeds are calculated could explain some of the biases shown in Fig. 6. Globally, ACE is mainly increased in the 1.5°C stabilization scenario by the increase in the number of intense tropical cyclones. Increases in average storm duration also lead to in the increase in ACE. However, as the total number of storms is significantly decreased in the 2.0°C stabilization scenario, ACE is decreased compared to the cooler stabilization scenario. The global changes

are dominated by similar changes in the North Atlantic and Northeast Pacific. Changes in the Northwest Pacific do not exhibit large changes but CAM5 has a significant cyclogenesis location bias in the Pacific Ocean that may be relevant. While the total number of simulated North Pacific storms is a reasonable representation of observations (Wehner et al., 2014), Northwestern Pacific storms originate too far to the east, causing cyclogenesis and track densities to be too high in the central Pacific; this is the focus of current research to be presented elsewhere. Also of note is that ACE in the Southern Hemisphere does not change despite the cyclogenesis and track changes discussed above.

Figure 7 shows the relationship between peak wind speeds and central pressure minima at the time of maximum intensity for the three HAPPI ensembles. As there are no changes to the model configuration among the simulations other than forcing conditions, this relationship does not significantly change other than the appearance of combinations of wind speed and pressure at the very highest simulated intensities in the warmer simulations that do not occur in the historical simulation. The peak wind speed and central pressure minima relationship is controlled by the mechanical constraints of gradient wind balance, storm size and Coriolis force (Chavas et al., 2017; Chavas, private communication, October 2017). The small poleward shift in the track density (Fig. 5) and subtle structural changes in wind speed radii discussed below are not large enough to change this relationship. Warmer temperatures do change the distribution of peak wind speeds and central pressure minima (Fig. 3) but do not

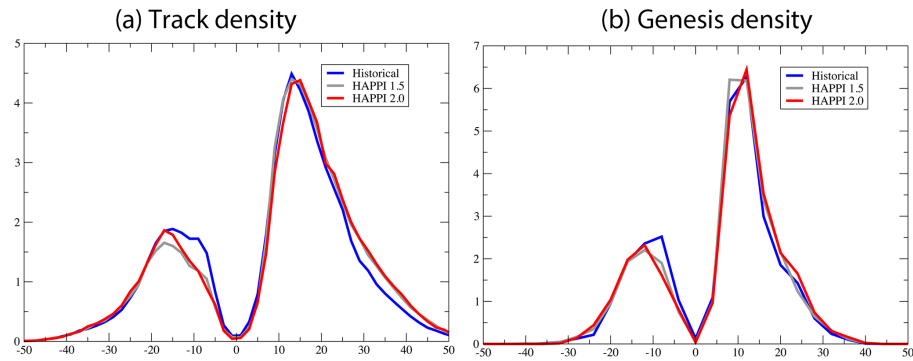


Figure 5. (a) Zonally averaged normalized tropical storm track density for the HAPPI scenarios. (b) Zonally averaged normalized tropical storm genesis density for the HAPPI scenarios. Blue: historical. Gray: 1.5° stabilization. Red: 2.0° stabilization.

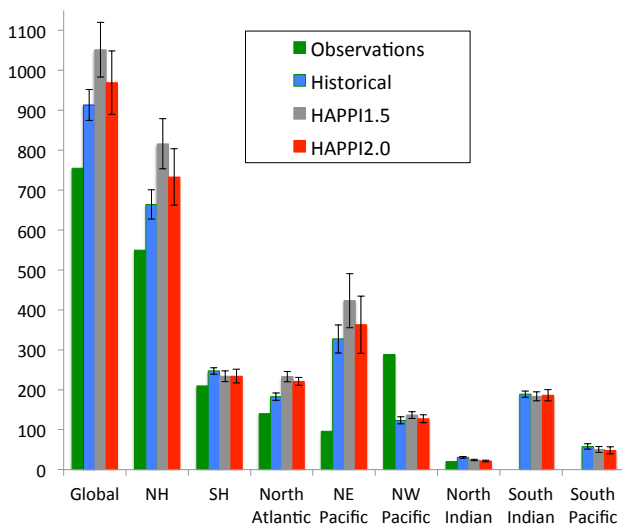


Figure 6. Average annual accumulated cyclonic energy (ACE) for the historical and HAPPI stabilization scenarios for all named storms by basin and globally for intense tropical cyclones only. Units: 1 ACE = 10^4 knots. Green: observations. Blue: historical. Gray: 1.5° stabilization. Red: 2.0° stabilization. Error bars are standard errors based on interannual variability.

appear to substantially change how they co-vary. We note, however, that model resolution and structure may influence the simulation of this relationship, thus requiring that evaluation of the effect of forcing changes on tropical storm statistics only be done with simulations from the same version of the climate model.

A definition of the physical size of tropical storms has recently been developed by Chavas et al. (2015) by defining an approximate radius at specified wind speeds. Figure 8 shows average Chavas radii for the historical and HAPPI stabilization scenarios. Radii are calculated every 3 h over the duration of every tracked storm for the threshold wind speeds defining the Saffir–Simpson categories and for the storm maximum wind speeds. Each relevant radius is cal-

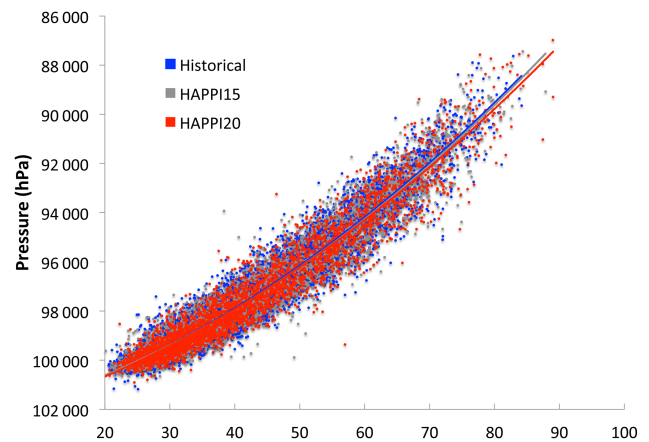


Figure 7. Scatterplot of minimum central pressure (hPa) versus maximum wind speed ($m s^{-1}$) at the time of maximum intensity for the HAPPI simulations. Blue: historical. Gray: 1.5° stabilization. Red: 2.0° stabilization. Solid lines are quadratic fits to the data.

culated for all storms. For instance, we calculate six Chavas radii for a category 5 storm (one for each Saffir–Simpson threshold) as all six Saffir–Simpson wind speeds are present at some point in such storms. Likewise, only a single Chavas radius for a category 0 storm and the higher wind speeds are not realized. The CAM5 HAPPI simulations exhibit about a 5% increase in category 0 Chavas radii and a smaller (2–3%) increase in category 1 Chavas radii in the warmer stabilized climates. Little change in Chavas radii is simulated for more intense wind speeds except for category 5 storms in the 2°C stabilization scenario that experience an 8% increase in Chavas radius. The increase in weak-wind-speed Chavas radii may be due to the change in the track density discussed above. The increased tracked tropical storms at higher latitudes are likely to be in the lower categories and may be starting their extratropical transition but still maintaining high winds. The increase in category 5 Chavas radii in only the warmer of the two HAPPI stabilizations currently lacks an explanation. Planned simulations of this version of

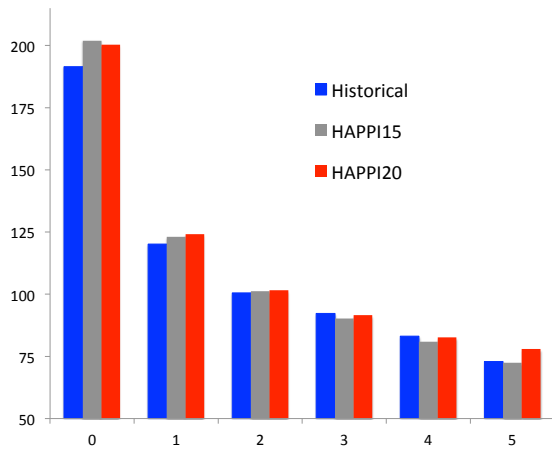


Figure 8. Chavas radii at different wind speeds selected as the definitions of the Saffir–Simpson categories (km) for the HAPPI simulations. Blue: historical. Gray: 1.5° stabilization. Red: 2.0° stabilization.

CAM5 with the so-called unHAPPI protocols (stabilized at 3 and 4 °C above preindustrial levels) may provide some insight into these aspects of change in storm structure.

3 Conclusions

The Half a degree Additional warming, Prognosis and Projected Impacts (HAPPI) experimental protocol was designed to rapidly inform the Intergovernmental Panel on Climate Change about the differences between stabilized climate at 1.5 and 2.0 °C above preindustrial global temperatures. However, it does not isolate all of the effects of forcing changes required to stabilize the climate from the present day conditions. In particular, the effect of sulfate aerosol reductions in the atmosphere has a nonlocal effect in the HAPPI simulations and has been demonstrated to be important to assessing changes in tropical cyclones (Huff et al., 2017) and heat waves (Wehner et al., 2017b). As the radiative forcing changes due to CO₂ between the historical and 1.5 °C scenarios may be smaller than the forcing changes due to aerosols, the CO₂ effects in tropical storms may be comparable or even smaller due to the aerosol effects at this stabilization level.

It is fair to say that the simulated differences in tropical cyclone statistics between the 1.5 and 2.0 °C stabilization scenarios as defined by the HAPPI protocols are small. Indeed, both warmer climates produce fewer tropical storms over all intensities in the global sense and the reduction increases as the sea surface temperature (SST) becomes warmer. Also, the most intense storms become more intense in both warmer SST configurations with the highest peak wind speeds and lowest central pressure minima simulated in the warmer of the two stabilizations.

Given the similarities between the two HAPPI scenarios and the importance of aerosol forcings, a more complete un-

derstanding of tropical storm frequency in aggressively stabilized climates requires detailed descriptions of the changes in those forcings. This would be particularly critical in geo-engineering schemes relying on solar radiation management. However, as found by Bacmeister et al. (2018) in their comparison of RCP4.5 to RCP8.5, major uncertainties in the pattern of SST changes also pose a significant challenge in accurately projecting future tropical storm frequency.

Changes in other important characteristics of tropical cyclone behavior are subtler. Both warmer climate conditions considered here project significant changes in the poleward density of tropical storm tracks compared to the historical simulations, but the differences between them are not likely to be highly significant. Also, changes in accumulated cyclonic energy (ACE), storm duration, track length and translational speed are complex with the differences clearly evident for only the most intense storms. Finally, some properties of tropical cyclones are not significantly altered in warmer climates, most notably the robust relationship between maximum wind speeds and central pressure minima.

Data availability. The tracking software used in this study is the Toolkit for Extreme Climate Analysis (TECA2.) available for download and installation at <https://github.com/LBL-EESA/TECA>. Data for this study total 23 TB and are currently available for download from the tape storage archive at the National Energy Research Supercomputing Center via anonymous wget scripts provided via the following DOI link: https://doi.org/10.25342/HAPPI_TC_2018. Because of the large dataset size, wget transfers of the entire database will likely be slow, and interested parties should contact the authors for faster access. As data transfer technologies serving this database evolve, faster alternatives will be offered via the DOI link.

The Supplement related to this article is available online at <https://doi.org/10.5194/esd-9-187-2018-supplement>.

Competing interests. The authors declare that they have no conflict of interest.

Special issue statement. This article is part of the special issue “The Earth system at a global warming of 1.5 °C and 2.0 °C”. It is not associated with a conference.

Acknowledgements. The work at LBNL was supported by the Regional and Global Modeling Program as part of the Calibrated and Systematic Characterization, Attribution, and Detection of Extremes project (CASCADE). LBNL is operated for the Department of Energy’s Office of Science under contract number DE-AC02-05CH11231. This document was prepared as an account of work

sponsored by the United States Government. While this document is believed to contain correct information, neither the United States Government nor any agency thereof, nor the Regents of the University of California, nor any of their employees, makes any warranty, express or implied, or assumes any legal responsibility for the accuracy, completeness, or usefulness of any information, apparatus, product, or process disclosed, or represents that its use would not infringe privately owned rights. Reference herein to any specific commercial product, process, or service by its trade name, trademark, manufacturer, or otherwise, does not necessarily constitute or imply its endorsement, recommendation, or favoring by the United States Government or any agency thereof, or the Regents of the University of California. The views and opinions of authors expressed herein do not necessarily state or reflect those of the United States Government or any agency thereof or the Regents of the University of California.

Work at Stony Brook University was supported by the Department of Energy's Office of Science under contract number DE-SC0016605.

These simulations were performed using resources of the National Energy Research Scientific Computing Center, a DOE Office of Science User Facility supported by the Office of Science of the US Department of Energy, also under contract no. DE-AC02-05CH11231.

Edited by: Ben Kravitz

Reviewed by: two anonymous referees

References

- Bacmeister, J. T., Wehner, M. F., Neale, R. B., Gettelman, A., Hannay, C., Lauritzen, P. H., Caron, J. M., and Truesdale, J. E.: Exploratory High-Resolution Climate Simulations using the Community Atmosphere Model (CAM), *J. Climate*, 27, 3073–3099, <https://doi.org/10.1175/JCLI-D-13-00387.1>, 2014.
- Bacmeister, J. T., Reed, K. A., Hannay, C., Lawrence, P. J., Bates, S. C., Truesdale, J. E., Rosenbloom, N. A., and Levy, M. N.: Projected changes in tropical cyclone activity under future warming scenarios using a high-resolution climate model, *Clim. Change*, 146, 547–560, <https://doi.org/10.1007/s10584-016-1750-x>, 2018.
- Camargo, S. J.: Global and Regional Aspects of Tropical Cyclone Activity in the CMIP5 Models, *J. Climate*, 26, 9880–9902, <https://doi.org/10.1175/JCLI-D-12-00549.1>, 2013.
- Chavas, D. R., Lin, N., and Emanuel, K.: A model for the complete radial structure of the tropical cyclone wind field. Part I: Comparison with observed structure, *J. Atmos. Sci.*, 72, 3647–3662, <https://doi.org/10.1175/JAS-D-15-0014.1>, 2015.
- Chavas, D. R., Reed, K. A., and Knaff, J. A.: Physical understanding of the tropical cyclone wind-pressure relationship, *Nat. Comm.*, 8, 1–11, <https://doi.org/10.1038/s41467-017-01546-9>, 2017.
- Dunstone, N. J., Smith, D. M., Booth, B. B. B., Hermanson, L., and Eade, R.: Anthropogenic aerosol forcing of Atlantic tropical storms, *Nat. Geosci.*, 6, 534–539, <https://doi.org/10.1038/ngeo1854>, 2013.
- Emanuel, K. and Nolan, D. S.: Tropical cyclone activity and the global climate system, Preprints, 26th Conf. on Hurricanes and Tropical Meteorology, Miami, FL, Am. Meteorol. Soc., 240–241, 2004.
- Huff, J. J. A., Reed, K. A., Bacmeister, J. B., and Wehner, M. F.: Evaluating the Influence of CAM5 Aerosol Configuration on Simulated Tropical Cyclones in the North Atlantic, *J. Adv. Model. Earth Syst.*, in review, 2017.
- Kiehl, J. T., Schneider, T. L., Rasch, P. J., Barth, M. C., and Wong, J.: Radiative forcing due to sulfate aerosols from simulations with the National Center for Atmospheric Research Community Climate Model, Version 3, *J. Geophys. Res.*, 105, 1441–1457, <https://doi.org/10.1029/1999JD900495>, 2000.
- Knutson, T. R., Sirutis, J. J., Garner, S. T., Held, I., and Tuleya, R. E.: Simulation of the Recent Multidecadal Increase of Atlantic Hurricane Activity Using an 18-km-Grid Regional Model, *B. Am. Meteorol. Soc.*, 88, 1549–1565, <https://doi.org/10.1175/BAMS-88-10-1549>, 2007.
- Knutson, T. R., Sirutis, J. J., Zhao, M., Tuleya, R. E., Bender, M., Vecchi, G. A., Villarini, G., and Chavas, D.: Global Projections of Intense Tropical Cyclone Activity for the Late Twenty-First Century from Dynamical Downscaling of CMIP5/RCP4.5 Scenarios, *J. Climate*, 28, 7203–7224, <https://doi.org/10.1175/JCLI-D-15-0129.1>, 2015.
- Lin, S.-J.: A “vertically Lagrangian” finite-volume dynamical core for global models, *Mon. Weather Rev.*, 132, 2293–2307, 2004.
- Lin, S.-J. and Rood, R. B.: Multidimensional flux-form semi-Lagrangian transport scheme, *Mon. Weather Rev.*, 124, 2046–2070, 1996.
- Lin, S.-J. and Rood, R. B.: An explicit flux-form semi-Lagrangian shallow water model on the sphere, *Q. J. Roy. Meteorol. Soc.*, 123, 2477–2498, 1997.
- Liu, M., Vecchi, G. A., Smith, J. A., and Murakami, H.: The Present-Day Simulation and Twenty-First-Century Projection of the Climatology of Extratropical Transition in the North Atlantic, *J. Climate*, 30, 2739–2756, <https://doi.org/10.1175/JCLI-D-16-0352.1>, 2017.
- Massey, N.: Generating sea ice patterns and uncertainty from coupled climate models, *J. Geophys. Res.*, in preparation, 2018.
- Maue, R. N.: Recent historically low global tropical cyclone activity, *Geophys. Res. Lett.*, 38, L14803, <https://doi.org/10.1029/2011GL047711>, 2011.
- Mitchell, D., AchutaRao, K., Allen, M., Bethke, I., Beyerle, U., Ciavarella, A., Forster, P. M., Fuglested, J., Gillett, N., Hausteine, K., Ingram, W., Iversen, T., Kharin, V., Klingaman, N., Massey, N., Fischer, E., Schleussner, C.-F., Scinocca, J., Seland, Ø., Shiogama, H., Shuckburgh, E., Sparrow, S., Stone, D., Uhe, P., Wallom, D., Wehner, M., and Zaaboul, R.: Half a degree additional warming, prognosis and projected impacts (HAPPI): background and experimental design, *Geosci. Model Dev.*, 10, 571–583, <https://doi.org/10.5194/gmd-10-571-2017>, 2017.
- Reed, K. A., Bacmeister, J. T., Rosenbloom, N. A., Wehner, M. F., Bates, S. C., Lauritzen, P. H., Truesdale, J. E., and Hannay, C.: Impact of the dynamical core on the direct simulation of tropical cyclones in a high-resolution global model, *Geophys. Res. Lett.*, 42, 3603–3608, <https://doi.org/10.1002/2015GL063974>, 2015.
- Reynolds, R. W., Rayner, N. A., Smith, T. M., Stokes, D. C., and Wang, W. C.: An improved in situ and satellite {SST} analysis for climate, *J. Climate*, 15, 1609–1625, 2002.
- Stone, D. A., Christidis, N., Folland, C., Perkins-Kirkpatrick, S., Perlwitz, J., Shiogama, H., Wehner, M. F., Wolski, P., Cholia, S., Krishnan, H., Murray, D., Ang'elil, O., Beyerle, U., Ciavarella, A., Dittus, A., and Quan, X.-W.: Experiment design of the In-

- ternational CLIVAR C20C+ Detection and Attribution Project. Weather and Climate Extremes, in preparation, 2017.
- Walsh, K. J. E., Camargo, S., Vecchi, G., Daloz, A. S., Elsner, J., Emanuel, K., Horn, M., Lim, Young-K., Roberts, M., Patricola, C., Scoccimarro, E., Sobel, A., Strazzo, S., Villarini, G., Wehner, M., Zhao, M., Kossin, J., LaRow, T., Oouchi, K., Schubert, S., Wang, H., Bacmeister, J., Chang, P., Chauvin, F., Jablonowski, C., Kumar, A., Murakami, H., Ose, T., Reed, K., Saravanan, R., Yamada, Y., Zarzycki, C., Vidale, P.-L., Jonas, J., and Henderson, N.: Hurricanes and climate: the U.S. CLIVAR working group on hurricanes, *B. Am. Meteorol. Soc.*, 96, 997–1017, <https://doi.org/10.1175/BAMS-D-13-00242.1>, 2015.
- Wehner, M. F., Reed, K., Li, F., Prabhat, Bacmeister, J., Chen, C.-T., Paciorek, C., Gleckler, P., Sperber, K., Collins, W. D., Gettelman, A., and Jablonowski, C.: The effect of horizontal resolution on simulation quality in the Community Atmospheric Model, CAM5.1, *J. Model. Earth Syst.*, 06, 980–997, <https://doi.org/10.1002/2013MS000276>, 2014.
- Wehner, M. F., Prabhat, Reed, K., Stone, D., Collins, W. D., and Bacmeister, J.: Resolution dependence of future tropical cyclone projections of CAM5.1 in the US CLIVAR Hurricane Working Group idealized configurations, *J. Climate*, 28, 3905–3925, <https://doi.org/10.1175/JCLI-D-14-00311.1>, 2015.
- Wehner, M. F., Reed, K. A., and Zarzycki, C. M.: High-Resolution Multi-Decadal Simulation of Tropical Cyclones, Chapter 8 in *Hurricanes and Climate Change*, edited by: Collins, J. and Walsh, K., Springer, 187–207, 2017a.
- Wehner, M., Stone, D., Mitchell, D., Shiogama, H., Fischer, E., Graff, L. S., Kharin, V. V., Sanderson, B., and Krishnan, H.: Changes in extremely hot days under stabilized 1.5 °C and 2.0 °C global warming scenarios as simulated by the HAPPI multi-model ensemble, *Earth Syst. Dynam.*, submitted, 2017b.
- Zarzycki, C. M., Thatcher, D. R., and Jablonowski, C.: Objective tropical cyclone extratropical transition detection in high-resolution reanalysis and climate model data, *J. Adv. Model. Earth Syst.*, 9, 130–148, <https://doi.org/10.1002/2016MS000775>, 2017.